Chapter 16
Antiferromagnetic Skyrmions and Bimerons

Laichuan Shen, Xue Liang, Jing Xia, Xichao Zhang, Motohiko Ezawa, Oleg A. Tretiakov, and Yan Zhou

Abstract The topological spin textures, such as magnetic skyrmions and bimerons, are currently a hot topic in condensed matter physics. Magnetic skyrmions are swirling spin textures, which can be stabilized in chiral magnets with perpendicular magnetic anisotropy, while magnetic bimerons can be regarded as the counterpart of skyrmions in magnetic systems with in-plane anisotropy. Both magnetic skyrmions and bimerons have attracted a lot of attentions, because they have small size and low depinning current, and can be used as nonvolatile information carries in future spintronic devices. In this chapter, we mainly present and discuss recent original results about the magnetization dynamics of antiferromagnetic skyrmions and bimerons excited by currents and spatially non-uniform magnetic anisotropy. In addition, we also explore possible applications based on antiferromagnetic skyrmions and bimerons, and review some relevant results.

16.1 Introduction

Antiferromagnets are magnetically ordered spin systems, and antiferromagnetic materials are promising for building advanced spintronic devices [1–4]. Considering an antiferromagnet with two sublattices, its magnetization dynamics is governed by the Landau-Lifshitz-Gilbert (LLG) equations [5], which can also describe the dynamics of a ferromagnet. However, the dynamic equations of antiferromagnets are coupled via the exchange interaction between sublattices, causing that the motion equation of the order parameter is of second order with respect to time [2]. Thus, the

L. Shen · X. Liang · J. Xia · X. Zhang · Y. Zhou (✉)
School of Science and Engineering, The Chinese University of Hong Kong, Shenzhen 518172, Guangdong, China
e-mail: zhouyan@cuhk.edu.cn

M. Ezawa
Department of Applied Physics, The University of Tokyo, 7-3-1 Hongo, Tokyo 113-8656, Japan

O. A. Tretiakov
School of Physics, The University of New South Wales, Sydney 2052, Australia

dynamic behavior of antiferromagnets should be similar to that described by the classical Newton's kinetic equation, and antiferromagnets may have richer dynamics than ferromagnets. On the other hand, intrinsic resonance frequency of the ferromagnet is typically on the order of gigahertz, while for the antiferromagnet it has high resonance frequency (generally, terahertz) thanks to the presence of strong antiferromagnetic exchange fields [6]. Therefore, the antiferromagnet can be used as an oscillator to generate terahertz oscillation signal [7]. Additionally, the magnetic moments of antiferromagnetic sublattices are compensated, which leads to nearly zero stray fields and insensitivity to the perturbation due to magnetic fields. These advantages make antiferromagnets active in condensed matter physics.

Magnetic textures, such as domain wall [8–10], skyrmion [11–16], bimeron [17–21] and skyrmionium [22–25] have attracted a great deal of attention due to their rich physics and important applications in information storage and computing devices. In addition to ferromagnetic systems, these magnetic textures can exist in antiferromagnetic systems. Figure 16.1 shows the antiferromagnetic domain wall, bimeron, skyrmion and skyrmionium, where antiferromagnetic textures may have some advantages compared to ferromagnetic analogues. For example, the speed of a ferromagnetic domain wall is limited by the Walker breakdown [26]. However, for a domain wall in antiferromagnet, only when its speed is close to the spin wave velocity (it has a very high value, about 10 km/s [9]), the domain wall will undergo the speed limit. On the other hand, skyrmions are topologically protected spin textures that have been experimentally observed in chiral materials, for example, MnSi [27] and Pt/Co/MgO [28]. For a skyrmion in ferromagnet, it has an integer topological charge, so that the
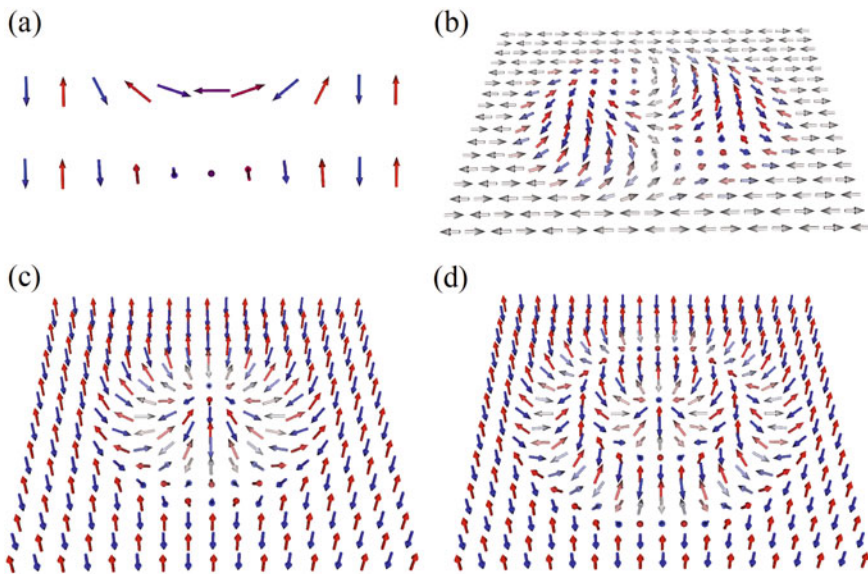

Fig. 16.1. Antiferromagnetic **a** domain wall, **b** bimeron, **c** skyrmion and **d** skyrmionium

Magnus force is always nonzero and leads to the skyrmion Hall effect [29, 30]. Such a skyrmion Hall effect may cause the skyrmion to annihilate at the sample edge, which is detrimental for practical applications. For an antiferromagnetic skyrmion, it consists of two ferromagnetic skyrmions (one on each sublattice) with opposite topological charges for magnetization, so that the net Magnus force is zero and the fast-moving skyrmion will not be destroyed by touching the sample edge.

In order to understand physics of antiferromagnetic textures and explore their applications, it is necessary to discuss their magnetization dynamics. In Sect. 16.2, we discuss the current-induced creation, motion and chaos of antiferromagnetic skyrmions and bimerons. In Sect. 16.3, we review and discuss of the spin torque nano-oscillators based on antiferromagnetic skyrmions. In Sect. 16.4, we focus on the study of synthetic antiferromagnetic skyrmions driven by the spin current. The following two parts, i.e., Sects. 16.5 and 16.6, mainly present and discuss the magnetization dynamics of antiferromagnetic skyrmions in the presence of spatially non-uniform magnetic anisotropy. In Sect. 16.5, we present the calculation results of using a magnetic anisotropy gradient to drive antiferromagnetic skyrmions, where the magnetic anisotropy gradient is applicable in both metals and insulators. Then, in Sect. 16.6, the pinning and depinning processes of antiferromagnetic skyrmions in a racetrack with a defect caused by the local variation of magnetic anisotropy are studied. Finally, in Sect. 16.7, we make a summary of this chapter.

16.2 Current-Driven Creation, Motion, and Chaos of Antiferromagnetic Skyrmions and Bimerons

In this section, we discuss the current-induced creation, motion and chaos of antiferromagnetic skyrmions and bimerons. Magnetic skyrmions are swirling spin textures carrying an integer topological charge, and they can be stabilized in chiral magnets with perpendicular magnetic anisotropy [11, 12]. Magnetic bimeron composed of two merons can be regarded as a counterpart of magnetic skyrmion in systems with in-plane magnetic anisotropy, which shares the merits of skyrmions, such as nanoscale size, nontrivial spin structure and low depinning current [18, 19]. These excellent characteristics make that both skyrmion and bimeron are promising candidates as information carriers in future spintronic devices. In practical applications, the controllable creation and manipulation of skyrmion and bimeron are crucial. In 2016, Zhang et al. [31] reported the creation of an antiferromagnetic skyrmion by applying a vertical spin current. In addition, their calculations show that using a junction geometry, the antiferromagnetic skyrmion is generated from a domain wall pair, as shown in Fig. 16.2. Similar to the skyrmion, an isolated bimeron is created in antiferromagnetic films by applying a vertical spin current to reverse the local magnetic moments, as reported by Shen et al. [19]. It is worth mentioning that in addition to the spin current, the time-dependent magnetic field can also induce the generation of an isolated antiferromagnetic skyrmion [32].
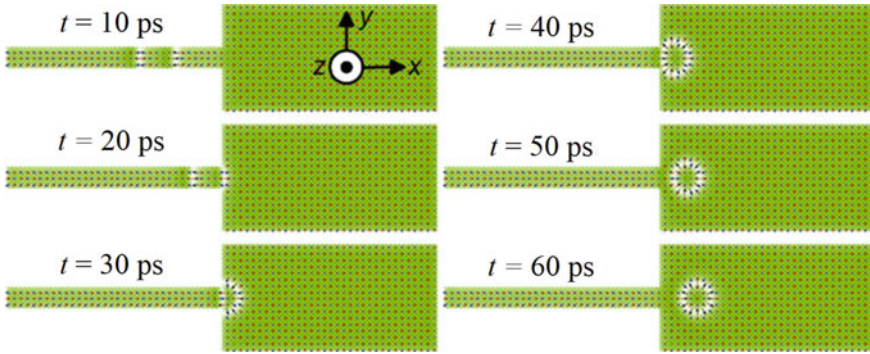
Fig. 16.2. Creation of an isolated antiferromagnetic skyrmion via a domain wall pair driven by a vertical spin current. Reprinted with permission from [31]. CC BY 4.0

On the other hand, manipulating magnetic textures is indispensable in future information storage and computing devices. Various methods have been proposed to drive antiferromagnetic skyrmion and bimeron, such as using spin currents [19, 31, 33, 34], magnetic anisotropy gradients [35] and temperature gradients [32]. In particular, the current-induced spin torque is a common way for manipulating magnetic materials. For current-induced spin-transfer torques including adiabatic and nonadiabatic terms [34, 36], the speed of both antiferromagnetic skyrmion and bimeron is proportional to the nonadiabatic spin-transfer torque parameter, and inversely proportional to the damping constant [33]. For current-induced damping-like spin torque [34], antiferromagnetic skyrmion and bimeron can be effectively driven to move, while for field-like spin torque, their response is weak because perfect antiferromagnetic materials are insensitive to a homogeneous magnetic field. Thanks to the cancellation of the Magnus force, current-induced spin torques can drive the antiferromagnetic skyrmion and bimeron at a speed of a few kilometers per second without showing any transverse drift, so that their motion trajectory is a perfect straight line along the driving force direction and they are ideal information carriers in racetrack-type memory [19, 25, 31, 33]. Note that in the high-speed region, a transverse expansion will be present, as reported in [33, 37, 38]. In 2020, Salimath et al. [37] demonstrated that such an expansion is reminiscent of the well-known Lorentz contraction, which has been identified in antiferromagnetic domain walls [9].

Next, based on the equation of motion, the dynamics of antiferromagnetic bimeron (or skyrmion) induced by the alternating current is discussed. As mentioned earlier, for antiferromagnetic systems, the motion equation of the order parameter is related to the second derivative with respect to time. On the other hand, the motion equation of the systems, such as the Landau-Lifshitz-Gilbert equation [5], is usually nonlinear, resulting in the dynamic behavior being complex or even chaotic. Thus, considering a skyrmion or bimeron in an antiferromagnetic nanodisk, its motion can be described by the Duffing equation, where the nanodisk boundary provides a nonlinear restoring force [19]. Note that for the chaos, the nonlinearity is a necessary

condition rather than a sufficient condition, so that not all nonlinear systems will exhibit chaotic behavior. Therefore, under the action of the alternating current, the antiferromagnetic bimeron (or skyrmion) generally does periodic motion. Taking certain parameter values, it shows chaotic behavior. The Lyapunov exponents (LEs) are usually used to judge whether there is chaos [39]. If the largest LE is positive, it means that two close trajectories will be separated. Namely, a small initial error will increase rapidly, resulting in the motion of antiferromagnetic bimeron being sensitive to initial conditions, and its motion behavior cannot be predicted for a long time, i.e., the bimeron does chaotic motion. In 2020, based on the motion equation of an antiferromagnetic bimeron (i.e., the Duffing equation), Shen et al. [19] calculated the bifurcation diagram and LEs, as shown in Fig. 16.3. It can be seen that the periodic and chaotic windows appear at intervals and a small damping constant can lead to the chaotic motion. In addition, the current is also of great importance to induce the occurrence of the chaos, as it can be easily tuned in experiment. Their calculation shows that for small currents, the system exhibits a periodic motion. With increasing currents, the period-doubling phenomenon takes place, and then the system shows chaotic behavior. It is worth mentioning that the chaotic behavior reported by Shen et al. [19] is subject to the boundary-induced restoring force, which depends on both the geometric and magnetic parameters. Since the antiferromagnetic bimerons show chaotic behavior, they can be used as chaotic oscillators, which are promising for various applications, such as detecting weak signals [40], generating random numbers [41] and building chaotic logic gates [42].
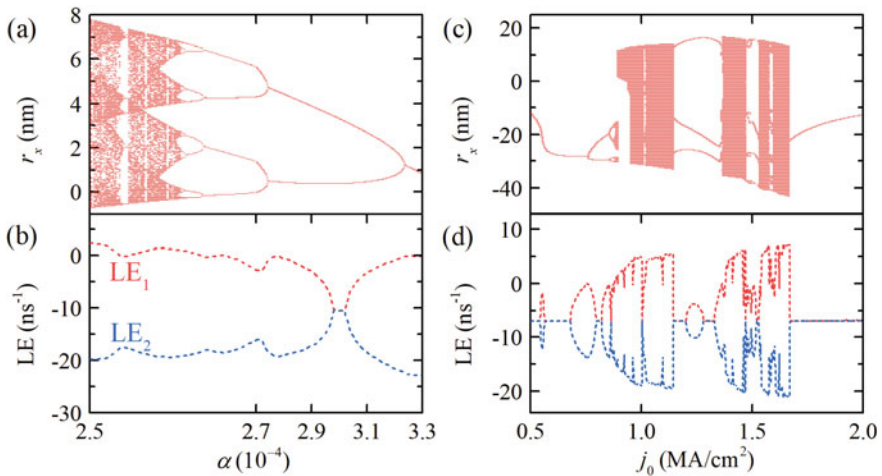

Fig. 16.3. a Calculated bifurcation diagram and **b** Lyapunov exponents (LEs) as functions of the damping constant. **c** Calculated bifurcation diagram and **d** LEs as functions of the current. Reprinted with permission from [19]. Copyright © 2020 American Physical Society

16.3 Spin Torque Nano-oscillators Based on Antiferromagnetic Skyrmions

The antiferromagnetic textures can be used not only as chaotic oscillators, but also as microwave signal generators (or spin torque nano-oscillators). In this section, we first review recent advances in skyrmion-based spin torque nano-oscillators, and then focus on the discussion of the nano-oscillators based on antiferromagnetic skyrmions. Spin torque nano-oscillators based on magnetic skyrmions have received great attention, because they can excite microwave signals with small linewidth and are expected to improve the output power [43–46]. In addition, the arrays of such nano-oscillators can be used to perform the neuromorphic computing [47]. In 2015, Zhang et al. [45] firstly demonstrated that applying a uniform current to the nano-contact oscillators, the ferromagnetic skyrmion can be induced to move in a circular motion, and then an oscillating signal is obtained by detecting the skyrmion position and using the magnetoresistance effect. In 2016, Garcia-Sanchez et al. [44] showed an alternative skyrmion-based nano-oscillator, in which a fixed layer with a vortex magnetic configuration is used to generate the spin-polarized current with a vortex-like polarization.

Generally, for the ferromagnetic skyrmion-based nano-oscillators, the oscillation frequencies are low (about 1 gigahertz), because the fast-moving skyrmion results in the presence of a large Magnus force and then the skyrmion will be destroyed at the nanodisk edge. In order to overcome this obstacle, various methods have been proposed. For example, in 2019, Feng et al. [48] showed that the oscillation frequency can be increased by 75%, where the nanodisk edge is enhanced by applying high perpendicular magnetic anisotropy. In addition, modifying the profile of Dzyaloshinskii-Moriya interaction can also lead to the increase in oscillation frequency [49]. Besides, in 2020, Jin et al. [50] showed that creating an annular groove in the surface of the free layer, the frequency tunability of the nano-oscillators reaches to 15.63 GHz. However, the above methods require sophisticated reprocessing and are not favorable from the point of view of device applications. Shen et al. [51] proposed to use the circular motion of an antiferromagnetic skyrmion to create the oscillation signal, where sophisticated reprocessing is not required. In addition to the cancellation of the Magnus force, the antiferromagnetic skyrmion obeys the inertial dynamics, as the motion equation of the antiferromagnetic order parameter is of second order with respect to time (for ferromagnetic dynamic equation it is of first order). Thus, the motion behavior of the antiferromagnetic and ferromagnetic skyrmions in a nanodisk is different, and the oscillation frequency of the antiferromagnetic skyrmion (tens of gigahertz) is higher than that of the ferromagnetic skyrmion [51]. Figure 16.4 shows the comparison of ferromagnetic and antiferromagnetic skyrmion-based nano-oscillators. We can see that the ferromagnetic skyrmion moves toward the nanodisk center when the positive current is applied, while for the negative current, the skyrmion is destroyed at the nanodisk edge. For the antiferromagnetic skyrmion, it moves steadily in the nanodisk under the action of the same currents, and its motion is independent of the sign of the applied current.

Fig. 16.4. The comparison of ferromagnetic and antiferromagnetic skyrmions in the nanodisk. The trajectory for an antiferromagnetic skyrmion driven by positive (**a**) and negative (**b**) currents. The trajectory for a ferromagnetic skyrmion driven by positive (**c**) and negative (**d**) currents. Reprinted from [51], with the permission of AIP Publishing.
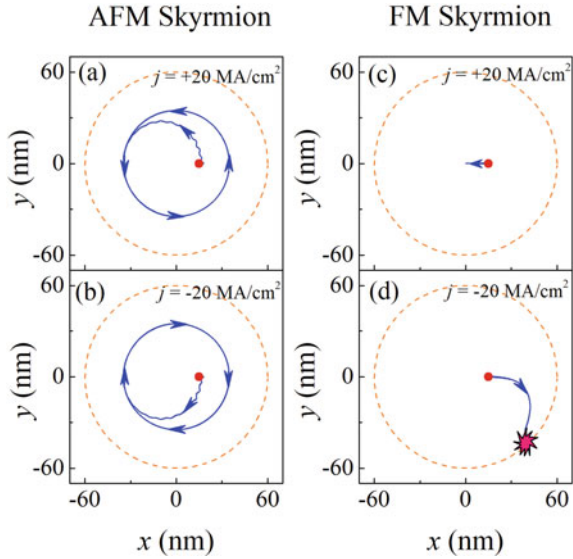
16.4 Synthetic Antiferromagnetic Skyrmions Driven by the Spin Current

In this section, we review and discuss the current-driven dynamics of magnetic skyrmions in the synthetic antiferromagnetic system. Different from the above-mentioned antiferromagnetic system, the synthetic antiferromagnet is made of ferromagnetic thin films but with antiferromagnetic interlayer exchange couplings [52, 53], which can be realized by the Ruderman-Kittel-Kasuya-Yosida (RKKY) interaction mechanism [54]. A basic and simple synthetic antiferromagnetic system can be constructed by a bilayer structure consisting of two antiferromagnetically exchange-coupled ferromagnetic layers with identical material properties and thicknesses. Namely, the total net magnetization of the bilayer system is equal to zero, leading to the zero-stray-field nature of a perfect antiferromagnetic thin film. It should be noted that an ultra-thin metal spacer is usually sandwiched between the two ferromagnetic layers, of which the thickness is adjusted to give rise to the RKKY-type interlayer antiferromagnetic exchange coupling.

The concept of skyrmions in synthetic antiferromagnets with zero net magnetization is originated for the purpose of eliminating the so-called skyrmion Hall effect [29, 30, 55]. The skyrmion Hall effect is a dynamic phenomenon associated with topological number of the skyrmion [29, 30], that is, a current-driven ferromagnetic skyrmion carrying an integer topological charge may experience a Magnus force and move at an angle with respect to the driving current direction. Such a phenomenon could result in the accumulation and/or even the destruction of skyrmions at sample edges, which is detrimental for some skyrmion-based applications such as the skyrmionic racetrack memory [52]. In a synthetic antiferromagnetic bilayer structure, such a
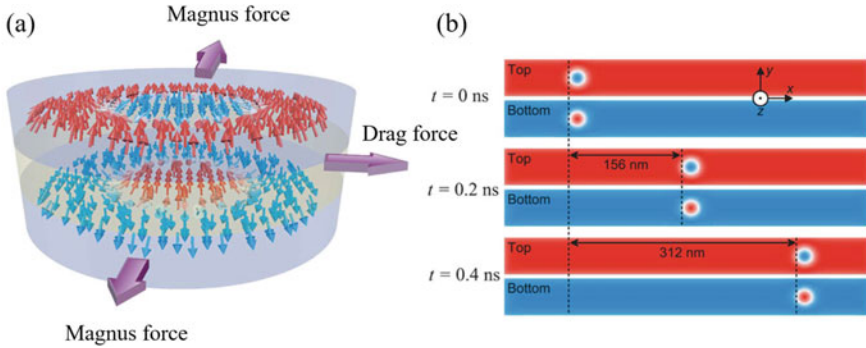
Fig. 16.5. A magnetic skyrmion in the synthetic antiferromagnetic bilayer system. **a** The Magnus forces acted on the top-layer and bottom-layer skyrmions will cancel each other, which results in the elimination of the skyrmion Hall effect. **b** Current-driven motion of a synthetic antiferromagnetic bilayer skyrmion. Reprinted with permission from [52]. CC BY 4.0

skyrmion Hall effect can be effectively eliminated as the skyrmions in the top and bottom layers have opposite skyrmion numbers and therefore, the Magnus forces acted on top and bottom skyrmions could cancel each other since they are identical in magnitude but pointing toward opposite directions, as shown in Fig. 16.5. Consequently, the synthetic antiferromagnetic bilayer skyrmion driven by a current moves in a straight line along the driving force direction, as shown in Fig. 16.5.

The concept of synthetic antiferromagnetic bilayer skyrmion was first purposed in a simulation work by Zhang et al. in 2016 [52]. In the same year, Zhang et al. also studied the skyrmion dynamics in multilayer synthetic antiferromagnetic racetracks [56]. It was found that the current-driven skyrmion shows no transverse motion in multilayer synthetic antiferromagnetic nanotracks packed with even identical ferromagnetic layers. Namely, only when the total skyrmion number equals zero and the system has zero net magnetization, the skyrmion Hall effect is truly eliminated. Zhang et al. [56] also suggest that the synthetic antiferromagnetic skyrmion may have a better thermal stability during its motion in nanotracks due to the absence of skyrmion-edge interaction induced by the skyrmion Hall effect. In 2017, by using micromagnetic simulations Tomasello et al. [57] further studied the performance of racetrack memory based on the synthetic antiferromagnetic skyrmion. They pointed out that the velocity of synthetic antiferromagnetic skyrmions and synthetic antiferromagnetic Néel-type domain walls are of the same order and can reach values larger than 1200 m/s, which is promising for real applications.

It is worth mentioning that the formation and current-induced motion of synthetic antiferromagnetic skyrmion bubbles have been realized in experiments by Dohi et al. in 2019 [58] and the stabilization of antiferromagnetic skyrmions in synthetic antiferromagnets at room temperature has also been experimentally realized by Legrand et al. in 2020 [59]. The two experimental works demonstrated promising features of synthetic antiferromagnetic skyrmions, that is, the thermal stable nanoscale size and negligible skyrmion Hall effect, which highlight the possibility of using synthetic

antiferromagnetic skyrmions in future high-performance spintronic devices with higher storage density and operation speed.

16.5 Antiferromagnetic Skyrmions Driven by the Magnetic Anisotropy Gradient

Previous section shows that antiferromagnetic skyrmions can be driven by electric currents. However, using the electric current as a driving source faces the issue of Joule heating, and the dynamics of the insulating antiferromagnet cannot be excited by an electric current. Therefore, alternative methods are crucial and have been explored, for example, using a voltage-controlled magnetic anisotropy gradient. The voltage-controlled magnetic anisotropy gradient is a promising method to drive the magnetic textures, because it has ultralow power consumption and is applicable in both metals and insulators. Recent studies experimentally and theoretically demonstrate that such a voltage-controlled magnetic anisotropy gradient can be used to manipulate the magnetic textures [35, 60–63]. Particularly, in 2019, Ma et al. [60] experimentally presented the electric field-induced creation and motion of domain walls and skyrmion bubbles. In this section, we first describe the calculation results of using a magnetic anisotropy gradient to drive antiferromagnetic skyrmions, and then compare the velocities of antiferromagnetic and ferromagnetic skyrmions.
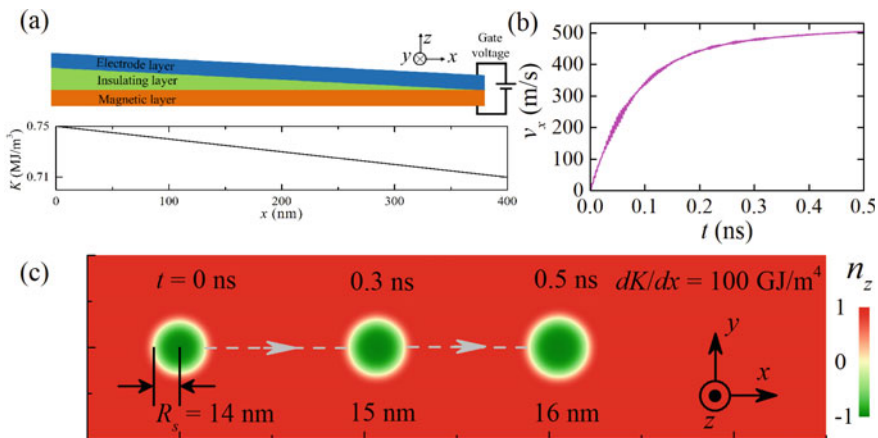

Fig. 16.6. **a** The sketch of the voltage-controlled magnetic anisotropy device, where the magnetic anisotropy K linearly decreases with the increase of the spatial coordinate x. **b** The evolution of the skyrmion speed for an antiferromagnetic skyrmion induced by a magnetic anisotropy gradient $dK/dx = 100$ GJ/m^4. **c** The top view of the antiferromagnetic skyrmion motion, where the color represents the out-of-plane component n_z of the Néel vector. Reprinted with permission from [35]. Copyright © 2018 American Physical Society

As shown in Fig. 16.6a, the magnetic anisotropy gradient ($dK/dx = 100$ GJ/m^4) is assumed to be induced by applying a voltage to the sample with a wedged insulating layer. Taking such an anisotropy gradient, i.e., $dK/dx = 100$ GJ/m^4, the motion of the antiferromagnetic skyrmion is simulated by solving the dynamic equation of antiferromagnet, and the time evolution of the skyrmion speed v_x is shown in Fig. 16.6b. We can see that the antiferromagnetic skyrmion is first accelerated to 450 m/s in 0.2 ns and then its speed increases slowly to 504 m/s by $t = 0.5$ ns [35]. The speed cannot reach a constant value, as the decreasing magnetic anisotropy K gives rise to the change of the skyrmion size. Namely, when the skyrmion moves in the positive x direction, the decreasing K results in the increase of the skyrmion size, so that the skyrmion speed will increase slowly. Fig. 16.6c shows the top view of the skyrmion motion, from which we can see that the radius of the skyrmion at $t = 0.5$ ns is larger than that of the initial state. Such an effect also exists in the case of ferromagnetic skyrmions driven by an anisotropy gradient, as reported by Tomasello et al. [62].

On the other hand, in antiferromagnetic systems, the magnetic moments of sublattices are compensated, so that the antiferromagnetic skyrmions do not show the skyrmion Hall effect [29, 30] due to zero net Magnus force. However, for ferromagnetic skyrmions, there is a transverse drift, i.e., the skyrmion Hall effect. Therefore, the motion behaviors of antiferromagnetic skyrmions driven by an anisotropy gradient are different from that of ferromagnetic skyrmions. The velocities of antiferromagnetic and ferromagnetic skyrmions are calculated as functions of the magnetic anisotropy gradient dK/dx and damping constant α, as shown in Fig. 16.7. It can be seen that their velocities are proportional to dK/dx and $1/\alpha$, and owing to the cancellation of the Magnus force, the speed of an antiferromagnetic skyrmion is larger than that of a ferromagnetic skyrmion.
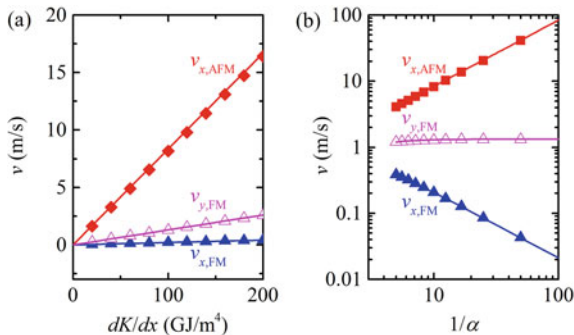

Fig. 16.7. Numerical (symbols) and analytical (lines) velocities of the antiferromagnetic and ferromagnetic skyrmions. **a** The velocities as functions of magnetic anisotropy gradient dK/dx, where the damping constant is set as 0.1. **b** The velocities as functions of the damping constant, where the magnetic anisotropy gradient dK/dx is 100 GJ/m^4. Reprinted with permission from [35]. Copyright © 2018 American Physical Society

As a result, adopting the magnetic anisotropy gradient to drive the skyrmion in pure antiferromagnets, the skyrmion can move at high speeds (up to 500 m/s) without any transverse drift. It is worth mentioning that using the anisotropy gradient as a driving source can be introduced to antiferromagnetically coupled bilayer systems, as reported by Qiu et al. [64]. The above results may open an alternative way for the design of antiferromagnetic skyrmion-based devices, such as the horizontal racetrack-type memory [65]. In addition, when these devices are chained together, it can also be used to build the antiferromagnetic skyrmion-based diode [66].

16.6   Pinning and Depinning of Antiferromagnetic Skyrmions

To understand more antiferromagnetic skyrmion physics and use it in future nanoscale magnetic data storage and logic devices, it is essentially important to know the pinning and depinning of antiferromagnetic skyrmions to defects. In this section, we discuss the effect of defects caused by the local variation of perpendicular magnetic anisotropy on the current-induced dynamics of an antiferromagnetic skyrmion under the framework of micromagnetics.

From [67], the local magnetic anisotropy value in the defect area is specified by $K = K_0\big[1.0 + \lambda/\exp(|\mathbf{r} - \mathbf{r}_d|/R_d)^2\big]$, where K_0 is the magnetic anisotropy constant in the homogeneous area, $|\lambda|$ denotes the amplitude of variation referred as the strength of the defect, R_d represents its characteristic size (i.e., the radius) and $\mathbf{r}_d$ is the position vector of the defect center. Such an anisotropy profile to describe the inhomogeneity induced by potential impurity sites, might be more realistic than a simple step-like defect or a defect with a linear variation of anisotropy, and is analogous to the model proposed by Kronmüller [68]. In addition, similar distribution of exchange interaction J_{ex} has also been used to discuss the skyrmion-defect interaction in ferromagnetic film [69, 70]. In all simulations, the coordinate of the antiferromagnetic skyrmion center is represented by (R_x, R_y) with the initial position (0, 0).

First let us consider the effect of the defect on the antiferromagnetic skyrmion without any external driving force. The simulation results show that when the skyrmion is placed at the area where the defect can interact with it, the skyrmion will spontaneously move and eventually stop at the center or off-center of the defect. Moreover, for the same defect, the skyrmion always be pinned at the same position. In particular, the final pinned position depends strongly on the ratio of skyrmion size to the defect size and is not sensitive to the strength of the defect. As shown in Fig. 16.8a, when the radius R_d of defect is smaller than the antiferromagnetic skyrmion radius R_{sk}, the skyrmion stops at the off-center of the defect, and the distance L gradually decreases as R_d increases. When R_d is close to or exceeds R_{sk}, L drops sharply and approaches 0, and the skyrmion will stay at the center of the defect. Such dynamic pinning processes are also similar to those of ferromagnetic skyrmions [71].
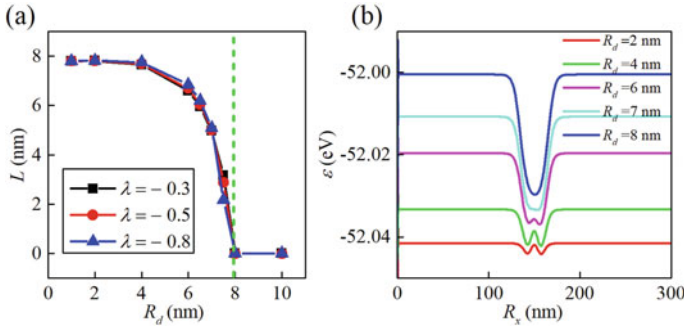
Fig. 16.8. a The distance L between the skyrmion final position and the defect center, as a function of the radius of defect for different strengths, where the green dashed line represents the radius of skyrmion; **b** The variation of the total energy with the skyrmion position R_x (with $R_y = 0$ nm) is plotted for different defect sizes, where the defect is initially placed at 150 nm in front of the skyrmion. Reprinted with permission from [67]. Copyright © 2019 American Physical Society.

To understand the physics behind the dynamic pinning process of the antiferromagnetic skyrmion mentioned above, Fig. 16.8b shows the total energy of the system vs the skyrmion position when the strength λ of the defect is fixed at –0.5. It can be found that there are two local minimal values near the defect center when $R_d < R_{sk}$, but only one minimal value at the center of defect when $R_d > R_{sk}$. Note that the skyrmion always prefers to be pinned at the low-energy place which related to the trough in the energy curve. Besides, for the defects with the same size and different strength (when $\lambda < 0$), the corresponding energy curves have the same shapes. Therefore, one can understand why the skyrmion final position is not sensitive to the strength of the defect, but mainly depends on its size.

We further discuss the motion of an antiferromagnetic skyrmion driven by the spin-polarized current in a defective racetrack, and find the transition from a pinned to a depinned state. Considering the force $\mathbf{F}_u$ arising from the defect is obtained by $\mathbf{F}_u = -\nabla \varepsilon$ where $\varepsilon (R_x, R_y)$ is the total potential energy of the system, the dynamic behaviors of the antiferromagnetic skyrmion around defect will depend on both the driving current density and the defect. As shown in Fig. 16.9, four motion behaviors of the skyrmion will occur when $\lambda = -0.5$. It also can be found that for different defect sizes, there will always be a critical depinning current density j_c required to drive the skyrmion passing through the defect area successfully along a straight line. Reference [67] has shown that the critical current density not only increases with increasing defect strength, but also is proportional to the radius of the defect. Moreover, it is much larger than that of the homogeneous racetrack where $\lambda = 0$ ($\sim 10^6$ A m^{-2}), which implies that a proper understanding of how antiferromagnetic skyrmions interact with defects is vital for the development and performance of future spintronic devices.

Generally, the potential defects or impurities in real materials may also contribute to the local increase of the magnetic anisotropy value, or even cause changes in other magnetic parameters, such as the Heisenberg exchange stiffness and the
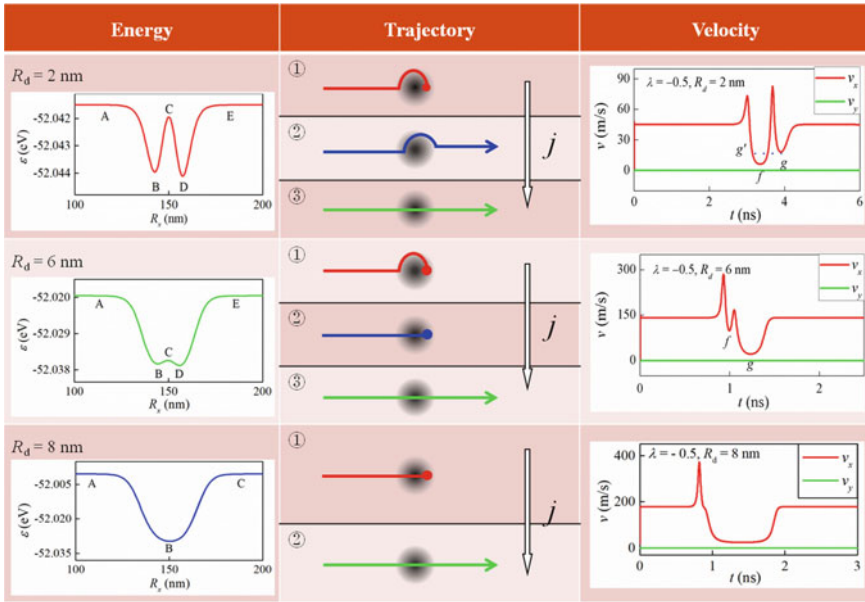
Fig. 16.9. Overview of the different motion behaviors of an antiferromagnetic skyrmion. Note that the black spot denotes the considered defect and the current density increases along the direction of the arrow. Reprinted with permission from [67]. Copyright © 2019 American Physical Society.

Dzyaloshinskii-Moriya interaction constant. Reference [67] has systematically investigated the dynamic pinning and depinning processes of antiferromagnetic skyrmions on a racetrack with different defects.

16.7 Summary

In this chapter, we have introduced and discussed the magnetization dynamics of antiferromagnetic skyrmions and bimerons excited by currents and spatially non-uniform magnetic anisotropy. In addition, we have also proposed possible applications based on antiferromagnetic skyrmions and bimerons, and reviewed some relevant results. We have shown that spin currents can create and drive the antiferromagnetic skyrmions and bimerons. Due to the cancellation of the Magnus force, the antiferromagnetic skyrmion and bimeron will not show the skyrmion Hall effect, so that they are ideal information carriers in racetrack-type memory. In addition, in the synthetic antiferromagnetic bilayer structure, the skyrmion also does not show the skyrmion Hall effect and moves along the driving force direction. Besides, we have demonstrated that the antiferromagnetic skyrmion can be driven by a magnetic anisotropy gradient. Also, we have studied the pinning and depinning processes of

antiferromagnetic skyrmions in a racetrack with a defect caused by the local variation of magnetic anisotropy. In addition to studying the dynamics of skyrmions in an antiferromagnetic racetrack, we also discussed the dynamic behavior of antiferromagnetic skyrmions in a nanodisk. In particular, we pointed out that driving an antiferromagnetic skyrmion to move in a circular motion on a nanodisk, one may get an oscillation signal with high frequencies (tens of gigahertz). These results are useful for understanding skyrmion and bimeron physics in antiferromagnetic systems, and may provide guidelines for building spintronic devices based on antiferromagnetic textures.

References

1. T. Jungwirth, X. Marti, P. Wadley, J. Wunderlich, Antiferromagnetic spintronics. Nat. Nanotechnol. **11**, 231 (2016)
2. V. Baltz, A. Manchon, M. Tsoi, T. Moriyama, T. Ono, Y. Tserkovnyak, Antiferromagnetic spintronics. Rev. Mod. Phys. **90**, 015005 (2018)
3. O. Gomonay, V. Baltz, A. Brataas, Y. Tserkovnyak, Antiferromagnetic spin textures and dynamics. Nat. Phys. **14**, 213 (2018)
4. L. Šmejkal, Y. Mokrousov, B. Yan, A.H. MacDonald, Topological antiferromagnetic spintronics. Nat. Phys. **14**, 242 (2018)
5. T.L. Gilbert, A phenomenological theory of damping in ferromagnetic materials. IEEE Trans. Magn. **40**, 3443 (2004)
6. F. Keffer, C. Kittel, Theory of antiferromagnetic resonance. Phys. Rev. **85**, 329 (1952)
7. R. Cheng, D. Xiao, A. Brataas, Terahertz antiferromagnetic spin hall nano-oscillator. Phys. Rev. Lett. **116**, 207603 (2016)
8. O. Gomonay, T. Jungwirth, J. Sinova, High antiferromagnetic domain wall velocity induced by Neel spin-orbit torques. Phys. Rev. Lett. **117**, 017202 (2016)
9. T. Shiino, S.H. Oh, P.M. Haney, S.W. Lee, G. Go, B.G. Park, K.J. Lee, Antiferromagnetic domain wall motion driven by spin-orbit torques. Phys. Rev. Lett. **117**, 087203 (2016)
10. E.G. Tveten, A. Qaiumzadeh, O.A. Tretiakov, A. Brataas, Staggered dynamics in antiferromagnets by collective coordinates. Phys. Rev. Lett. **110**, 127208 (2013)
11. Y. Zhou, Magnetic skyrmions: Intriguing physics and new spintronic device concepts. Natl. Sci. Rev. **6**, 210 (2019)
12. X. Zhang, Y. Zhou, K. Mee Song, T. E. Park, J. Xia, M. Ezawa, X. Liu, W. Zhao, G. Zhao, S. Woo, Skyrmion-electronics: writing, deleting, reading and processing magnetic skyrmions toward spintronic applications, J. Phys.: Condens. Matter **32**, 143001 (2019)

13. U.K. Rossler, A.N. Bogdanov, C. Pfleiderer, Spontaneous skyrmion ground states in magnetic metals. Nature **442**, 797 (2006)
14. N. Nagaosa, Y. Tokura, Topological properties and dynamics of magnetic skyrmions. Nat. Nanotechnol. **8**, 899 (2013)
15. A. Fert, N. Reyren, V. Cros, Magnetic skyrmions: advances in physics and potential applications. Nat. Rev. Mater. **2**, 17031 (2017)
16. K. Everschor-Sitte, J. Masell, R.M. Reeve, M. Kläui, Perspective: Magnetic skyrmions— Overview of recent progress in an active research field. J. Appl. Phys. **124**, 240901 (2018)
17. Y.A. Kharkov, O.P. Sushkov, M. Mostovoy, Bound states of skyrmions and merons near the Lifshitz point. Phys. Rev. Lett. **119**, 207201 (2017)
18. B. Göbel, A. Mook, J. Henk, I. Mertig, O.A. Tretiakov, Magnetic bimerons as skyrmion analogues in in-plane magnets. Phys. Rev. B **99**, 060407(R) (2019)
19. L. Shen, J. Xia, X. Zhang, M. Ezawa, O.A. Tretiakov, X. Liu, G. Zhao, Y. Zhou, Current-induced dynamics and chaos of antiferromagnetic bimerons. Phys. Rev. Lett. **124**, 037202 (2020)
20. X. Zhang, J. Xia, L. Shen, M. Ezawa, O.A. Tretiakov, G. Zhao, X. Liu, Y. Zhou, Static and dynamic properties of bimerons in a frustrated ferromagnetic monolayer. Phys. Rev. B **101**, 144435 (2020)
21. X.Z. Yu, W. Koshibae, Y. Tokunaga, K. Shibata, Y. Taguchi, N. Nagaosa, Y. Tokura, Transformation between meron and skyrmion topological spin textures in a chiral magnet. Nature **564**, 95 (2018)
22. X. Zhang, J. Xia, Y. Zhou, D. Wang, X. Liu, W. Zhao, M. Ezawa, Control and manipulation of a magnetic skyrmionium in nanostructures. Phys. Rev. B **94**, 094420 (2016)
23. F. Zheng, H. Li, S. Wang, D. Song, C. Jin, W. Wei, A. Kovacs, J. Zang, M. Tian, Y. Zhang, H. Du, R.E. Dunin-Borkowski, Direct Imaging of a zero-field target skyrmion and its polarity switch in a chiral magnetic nanodisk. Phys. Rev. Lett. **119**, 197205 (2017)
24. M. Finazzi, M. Savoini, A.R. Khorsand, A. Tsukamoto, A. Itoh, L. Duo, A. Kirilyuk, T. Rasing, M. Ezawa, Laser-induced magnetic nanostructures with tunable topological properties. Phys. Rev. Lett. **110**, 177205 (2013)
25. L. Shen, X. Li, Y. Zhao, J. Xia, G. Zhao, Y. Zhou, Current-induced dynamics of the antiferromagnetic skyrmion and skyrmionium. Phys. Rev. Appl. **12**, 064033 (2019)
26. N.L. Schryer, L.R. Walker, The motion of 180° domain walls in uniform dc magnetic fields. J. Appl. Phys. **45**, 5406 (1974)
27. S. Mühlbauer, B. Binz, F. Jonietz, C. Pfleiderer, A. Rosch, A. Neubauer, R. Georgii, P. Böni, Skyrmion lattice in a chiral magnet. Science **323**, 915 (2009)
28. O. Boulle, J. Vogel, H. Yang, S. Pizzini, D. de Souza Chaves, A. Locatelli, T. O. Mentes, A. Sala, L. D. Buda-Prejbeanu, O. Klein, M. Belmeguenai, Y. Roussigne, A. Stashkevich, S. M. Cherif, L. Aballe, M. Foerster, M. Chshiev, S. Auffret, I. M. Miron, G. Gaudin, Room-temperature chiral magnetic skyrmions in ultrathin magnetic nanostructures, Nat. Nanotechnol. **11**, 449 (2016)
29. W. Jiang, X. Zhang, G. Yu, W. Zhang, X. Wang, M. Benjamin Jungfleisch, John E. Pearson, X. Cheng, O. Heinonen, K. L. Wang, Y. Zhou, A. Hoffmann, Suzanne G. E. te Velthuis, Direct observation of the skyrmion Hall effect, Nat. Phys. **13**, 162 (2017)
30. K. Litzius, I. Lemesh, B. Krüger, P. Bassirian, L. Caretta, K. Richter, F. Büttner, K. Sato, O.A. Tretiakov, J. Förster, R.M. Reeve, M. Weigand, I. Bykova, H. Stoll, G. Schütz, G.S.D. Beach, M. Kläui, Skyrmion Hall effect revealed by direct time-resolved X-ray microscopy. Nat. Phys. **13**, 170 (2017)
31. X. Zhang, Y. Zhou, M. Ezawa, Antiferromagnetic skyrmion: Stability, creation and manipulation. Sci. Rep. **6**, 24795 (2016)
32. R. Khoshlahni, A. Qaiumzadeh, A. Bergman, A. Brataas, Ultrafast generation and dynamics of isolated skyrmions in antiferromagnetic insulators. Phys. Rev. B **99**, 054423 (2019)
33. J. Barker, O.A. Tretiakov, Static and dynamical properties of antiferromagnetic skyrmions in the presence of applied current and temperature. Phys. Rev. Lett. **116**, 147203 (2016)

34. H. Velkov, O. Gomonay, M. Beens, G. Schwiete, A. Brataas, J. Sinova, R.A. Duine, Phenomenology of current-induced skyrmion motion in antiferromagnets. New J. Phys. **18**, 075016 (2016)
35. L. Shen, J. Xia, G. Zhao, X. Zhang, M. Ezawa, O.A. Tretiakov, X. Liu, Y. Zhou, Dynamics of the antiferromagnetic skyrmion induced by a magnetic anisotropy gradient. Phys. Rev. B **98**, 134448 (2018)
36. K.M.D. Hals, Y. Tserkovnyak, A. Brataas, Phenomenology of current-induced dynamics in antiferromagnets. Phys. Rev. Lett. **106**, 107206 (2011)
37. A. Salimath, F. Zhuo, R. Tomasello, G. Finocchio, A. Manchon, Controlling the deformation of antiferromagnetic skyrmions in the high-velocity regime. Phys. Rev. B **101**, 024429 (2020)
38. C. Jin, C. Song, J. Wang, Q. Liu, Dynamics of antiferromagnetic skyrmion driven by the spin Hall effect. Appl. Phys. Lett. **109**, 182404 (2016)
39. Z. Yang, S. Zhang, Y.C. Li, Chaotic dynamics of spin-valve oscillators. Phys. Rev. Lett. **99**, 134101 (2007)
40. G. Wang, D. Chen, J. Lin, X. Chen, The application of chaotic oscillators to weak signal detection. IEEE Trans. Industr. Electron. **46**, 440 (1999)
41. A. Fukushima, T. Seki, K. Yakushiji, H. Kubota, H. Imamura, S. Yuasa, K. Ando, Spin dice: A scalable truly random number generator based on spintronics. Appl. Phys. Express **7**, 083001 (2014)
42. W.L. Ditto, A. Miliotis, K. Murali, S. Sinha, M.L. Spano, Chaogates: morphing logic gates that exploit dynamical patterns. Chaos **20**, 037107 (2010)
43. C. Jin, J. Wang, W. Wang, C. Song, J. Wang, H. Xia, Q. Liu, Array of synchronized nano-oscillators based on repulsion between domain wall and skyrmion. Phys. Rev. Appl. **9**, 044007 (2018)
44. F. Garcia-Sanchez, J. Sampaio, N. Reyren, V. Cros, J.V. Kim, A skyrmion-based spin-torque nano-oscillator. New J. Phys. **18**, 075011 (2016)
45. S. Zhang, J. Wang, Q. Zheng, Q. Zhu, X. Liu, S. Chen, C. Jin, Q. Liu, C. Jia, D. Xue, Current-induced magnetic skyrmions oscillator. New J. Phys. **17**, 023061 (2015)
46. Y. Zhou, E. Iacocca, A.A. Awad, R.K. Dumas, F.C. Zhang, H.B. Braun, J. Akerman, Dynamically stabilized magnetic skyrmions. Nat. Commun. **6**, 8193 (2015)
47. M. Zahedinejad, A.A. Awad, S. Muralidhar, R. Khymyn, H. Fulara, H. Mazraati, M. Dvornik, J. Akerman, Two-dimensional mutually synchronized spin Hall nano-oscillator arrays for neuromorphic computing. Nat. Nanotechnol. **15**, 47 (2020)
48. Y. Feng, J. Xia, L. Qiu, X. Cai, L. Shen, F.J. Morvan, X. Zhang, Y. Zhou, G. Zhao, A skyrmion-based spin-torque nano-oscillator with enhanced edge. J. Magn. Magn. Mater. **491**, 165610 (2019)
49. J.H. Guo, J. Xia, X.C. Zhang, P.W.T. Pong, Y.M. Wu, H. Chen, W.S. Zhao, Y. Zhou, A ferromagnetic skyrmion-based nano-oscillator with modified profile of Dzyaloshinskii-Moriya interaction. J. Magn. Magn. Mater. **496**, 165912 (2020)
50. C. Jin, Y. Ma, C. Song, H. Xia, J. Wang, C. Zhang, Z. Zeng, J. Wang, Q. Liu, High-frequency spin transfer nano-oscillator based on the motion of skyrmions in an annular groove. New J. Phys. **22**, 033001 (2020)
51. L. Shen, J. Xia, G. Zhao, X. Zhang, M. Ezawa, O.A. Tretiakov, X. Liu, Y. Zhou, Spin torque nano-oscillators based on antiferromagnetic skyrmions. Appl. Phys. Lett. **114**, 042402 (2019)
52. X. Zhang, Y. Zhou, M. Ezawa, Magnetic bilayer-skyrmions without skyrmion Hall effect. Nat. Commun. **7**, 10293 (2016)
53. J. Xia, X. Zhang, M. Ezawa, Z. Hou, W. Wang, X. Liu, Y. Zhou, Current-driven dynamics of frustrated skyrmions in a synthetic antiferromagnetic bilayer. Phys. Rev. Appl. **11**, 044046 (2019)
54. S.S. Parkin, R. Bhadra, K.P. Roche, Oscillatory magnetic exchange coupling through thin copper layers. Phys. Rev. Lett. **66**, 2152 (1991)
55. J. Zang, M. Mostovoy, J.H. Han, N. Nagaosa, Dynamics of Skyrmion crystals in metallic thin films. Phys. Rev. Lett. **107**, 136804 (2011)

56. X. Zhang, M. Ezawa, Y. Zhou, Thermally stable magnetic skyrmions in multilayer synthetic antiferromagnetic racetracks. Phys. Rev. B **94**, 064406 (2016)
57. R. Tomasello, V. Puliafito, E. Martinez, A. Manchon, M. Ricci, M. Carpentieri, G. Finocchio, Performance of synthetic antiferromagnetic racetrack memory: domain wall versus skyrmion. J. Phys. D: Appl. Phys. **50**, 325302 (2017)
58. T. Dohi, S. DuttaGupta, S. Fukami, H. Ohno, Formation and current-induced motion of synthetic antiferromagnetic skyrmion bubbles. Nat. Commun. **10**, 5153 (2019)
59. W. Legrand, D. Maccariello, F. Ajejas, S. Collin, A. Vecchiola, K. Bouzehouane, N. Reyren, V. Cros, A. Fert, Room-temperature stabilization of antiferromagnetic skyrmions in synthetic antiferromagnets. Nat. Mater. **19**, 34 (2020)
60. C. Ma, X. Zhang, J. Xia, M. Ezawa, W. Jiang, T. Ono, S.N. Piramanayagam, A. Morisako, Y. Zhou, X. Liu, Electric field-induced creation and directional motion of domain walls and skyrmion bubbles. Nano Lett. **19**, 353 (2019)
61. X. Wang, W.L. Gan, J.C. Martinez, F.N. Tan, M.B.A. Jalil, W.S. Lew, Efficient skyrmion transport mediated by a voltage controlled magnetic anisotropy gradient. Nanoscale **10**, 733 (2018)
62. R. Tomasello, S. Komineas, G. Siracusano, M. Carpentieri, G. Finocchio, Chiral skyrmions in an anisotropy gradient. Phys. Rev. B **98**, 024421 (2018)
63. H. Xia, C. Song, C. Jin, J. Wang, J. Wang, Q. Liu, Skyrmion motion driven by the gradient of voltage-controlled magnetic anisotropy. J. Magn. Magn. Mater. **458**, 57 (2018)
64. L. Qiu, J. Xia, Y. Feng, L. Shen, F.J. Morvan, X. Zhang, X. Liu, L. Xie, Y. Zhou, G. Zhao, Dynamics of antiskyrmions induced by the voltage-controlled magnetic anisotropy gradient. J. Magn. Magn. Mater. **496**, 165922 (2020)
65. S.S. Parkin, M. Hayashi, L. Thomas, Magnetic domain-wall racetrack memory. Science **320**, 190 (2008)
66. J. Wang, J. Xia, X. Zhang, G.P. Zhao, L. Ye, J. Wu, Y. Xu, W. Zhao, Z. Zou, Y. Zhou, Controllable transport of a skyrmion in a ferromagnetic narrow channel with voltage-controlled magnetic anisotropy. J. Phys. D: Appl. Phys. **51**, 205002 (2018)
67. X. Liang, G. Zhao, L. Shen, J. Xia, L. Zhao, X. Zhang, Y. Zhou, Dynamics of an antiferromagnetic skyrmion in a racetrack with a defect. Phys. Rev. B **100**, 144439 (2019)
68. H. Kronmüller, Theory of nucleation fields in inhomogeneous ferromagnets. Phys. Stat. Sol. B **114**, 385 (1987)
69. S.-Z. Lin, C. Reichhardt, C.D. Batista, A. Saxena, Particle model for skyrmions in metallic chiral magnets: Dynamics, pinning, and creep. Phys. Rev. B **87**, 214419 (2013)
70. Y. H. Liu, Y. Q. Li, A mechanism to pin skyrmions in chiral magnets, J. Phys.: Condens. Matter **25**, 076005 (2013)
71. D. Stosic, T.B. Ludermir, M.V. Milošević, Pinning of magnetic skyrmions in a monolayer Co film on Pt(111): Theoretical characterization and exemplified utilization. Phys. Rev. B **96**, 214403 (2017)